13th World Conference on Earthquake Engineering
Vancouver, B.C., Canada
August 1-6, 2004
Paper No. 1651

TIME-HISTORY RESPONSE ANALYSIS OF BOX SECTION STEEL FRAMES CONSIDERING THE EFFECT OF LOCAL BUCKLING

Noriko KODAMA[1], Yozo GOTO[2] and Teruhiko YODA[3]

SUMMARY

A time-history response analysis method for seismic diagnosis of existing box section steel frames in Japan is proposed and verified. The features of the method are: i) using direct time integration method, ii) using beam Finite Elements with stress-strain hysteresis model, iii) considering local buckling and iv) being alternative method of highly time-consuming FE analysis using shell elements.

Shell FE analyses showed that local buckling of existing box section steel frames occurs between transverse stiffeners. Therefore, the average stress-strain relation of the beam model can be formulated for transverse stiffener spacing. It is formulated as softening stress-strain relation after local buckling occurs. The buckling stress of flange was evaluated as the elasto-plastic buckling stress of a T-section column, whose array forms the flange, and that of web panel was evaluated as the elasto-plastic buckling stress of a simply supported panel.

The maximum lateral displacement and the residual displacement of an existing box section steel frame were well estimated by the proposed beam element model that considers the deterioration effect due to local buckling, while the calculation time is considerably shorter than that of a shell element model.

INTRODUCTION

After the disastrous Hyogoken-Nanbu earthquake in 1995, the Japan Society of Civil Engineers (JSCE [1]) proposed the two principal concepts for earthquake resistant design of infrastructures: i) ground motions used in earthquake resistant design are graded into two levels and ii) performance-based design should be adopted. The "Level II" earthquake motion is defined as a very strong motion that is generated in the near field of inland faults, and can cause severe plastic deformation of structures. Most of the

[1] Dr. Eng., Researcher, Kawasaki Laboratory, EDM, National Research Institute for Earth Science and Disaster Prevention, Kanagawa, Japan. Email: kodama@kedm.bosai.go.jp
[2] Dr. Eng., General Manager, Kawasaki Laboratory, EDM, National Research Institute for Earth Science and Disaster Prevention, Kanagawa, Kanagawa, Japan.
[3] Dr. Eng., Professor, School of Science and Engineering, Waseda University, Tokyo, Japan.

Japanese earthquake resistant design codes, such as the Design Specifications for Highway Bridges (Japan Road Association [2]), have been revised according to these concepts.
The revised design codes recommend that the earthquake ground motions, the numerical analysis models and the required-performance levels, which are regulated by the latest earthquake resistant design codes, are to be adopted. However, many problems in adopting performance-based design remain unsolved, and one of those is an evaluation method for dynamic behavior of steel structures in the post-peak range.

Simple evaluation methods such as the ductility design method (JSCE [3]), which is based on the equal energy assumption of an elastic and an elasto-plastic single degree-of-freedom structures (Newmark [4]), or the time-history response analysis method using the $M-\phi$ (beam moment-curvature) model (Oshima [5]), were proposed and have so far put into practical use. However, application of these simple methods to steel frames can not be rationalized, because steel frames have often complicated shapes and consequently multi degrees-of-freedom, and furthermore strong ground motion may cause steel frames severe inelastic deformation such as local buckling.

On the other hand, a $\sigma-\varepsilon$ (stress-strain) model is generally used as FEM analyses using beam elements, so that the structure to be analyzed can have any shape or carry any eccentric load (Isoe [6]). However, the $\sigma-\varepsilon$ model that can evaluate residual displacements of locally buckled steel rigid frames with adequate precision has not been established.

This paper proposes and verifies a time-history response analysis method for seismic diagnosis of existing steel rigid frames. The principal features of the method are as follows: i) using direct time integration method, ii) using stress-strain hysteresis model, iii) using elasto-plastic finite displacement analysis and beam Finite Elements, iv) considering local buckling of steel frames and v) being alternative method of highly time-consuming FE analysis using shell elements.

The maximum lateral displacement and the residual displacement will be predicted by this method. The method is intended to be used with steel frames which have i) box sections and ii) properly designed stiffeners which meet the past Design Specifications for Highway Bridges (Japan Road Association [7]).

LOCAL BUCKLING BEHAVIOR OF BOX SECTION STEEL PIERS

Local buckling shape

In order to establish a beam element ($\sigma-\varepsilon$) model that considers the effect of local buckling, time-history response analyses using shell FE analysis were performed for the local buckling problem of box section steel columns. The dimensions and the analysis parameters of box-section columns are shown in **Table 1**. Where, L=height of column, b =breadth, t =thickness, n =number of panels, a=distance between transverse stiffeners and N/N_y =axial load ratio, and the subscripts f = flange, w = web, r = longitudinal stiffener and d = transverse stiffener.

The analyses were carried out using ABAQUS/Standard Version 5.8 (Hibbitt, Karlsson & Sorensen, Inc. [8]). Four nodes linear general-purpose shell elements and kinematic hardening rule with strain hardening effect were used. In order to define material hysteresis models, the plots shown in **Fig. 1** were used for each steel type. Panels in stiffened plates were discretized into at least four elements breadthways. The acceleration history in NS direction during the Hyogoken-Nanbu earthquake observed by the Kobe Meteorological Observatory (hereafter referred to as JMA acceleration history, JSCE [10]) was imposed on column bases. In order to ensure that local bucking occurs, the axial load ratios N/N_y were set to 0.15 and larger.

Table 1 Dimensions and analysis parameters of the box-section columns

No.	L (mm)	Flange			Web			Long. stiffener		Transverse stiffener			N/N_y (%)	Steel type
		b_f (mm)	t_f (mm)	n_f	b_w (mm)	t_w (mm)	n_w	b_r (mm)	t_r (mm)	b_d (mm)	t_d (mm)	$a^\dagger$ (mm)		
C1	7650	2000	25	5	1700	25	4	170	19	250	16	2000	15	SM570
C2	5750	1700	19	4	1700	19	4	140	14	230	15	1500	15	SM490YA
C3	9500	2000	25	5	2500	29	5	140	14	270	17	1421	15	SM490YA
C4	8000	2500	16	6	2000	15	5	160	16	430	10	2000	15	SM490YA
C5	7500	2200	20	5	2000	21	4	210	20	350	10	2500	20	SM490YB
C6	6000	2000	40	5	2000	28	5	200	20	320	19	2000	15	SM570
C7	5400	1700	25	4	1700	16	4	140	14	230	15	1800	20	SM400A
C8	7400	2000	32	5	2000	28	5	200	20	320	19	1850	15	SM570
C9	6400	2200	22	5	2000	21	4	160	18	350	10	1600	15	SM490YB

† values at the bases

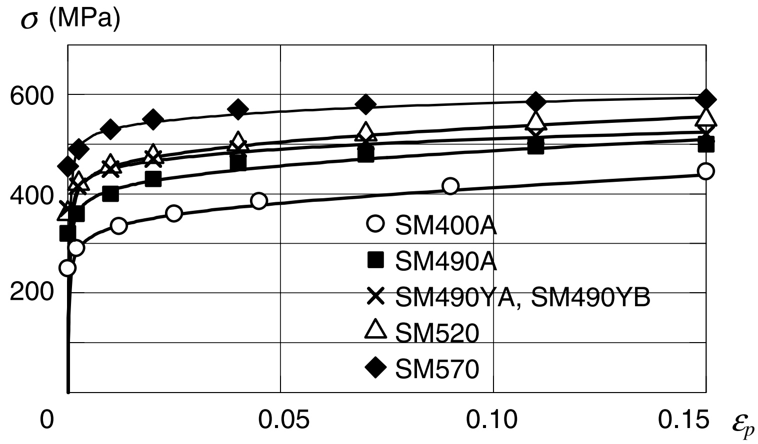

Fig. 1 Uniaxial stress σ − plastic strain ε_p relations of steel materials

Fig. 2 shows the example deformation shapes of the steel columns. It shows that flanges and webs buckle practically between the pier base and the nearest transverse stiffener from the base. This indicates that local buckling behavior can be estimated for transverse stiffener spacing.

Stress - strain relations after local buckling

It appears that approximate formulas for the mean axial stress - mean axial strain relation of locally buckled stiffener spacing can be derived from results of shell FE analyses. The mean axial stresses and strains are defined here as follows (**Fig. 3**):

$$\bar{\sigma}_f = \frac{N_f}{A_f}, \quad \bar{\sigma}_{wp} = \frac{N_{wp}}{A_{wp}} \qquad (1a), (1b)$$

$$\bar{\varepsilon}_f = \frac{\Delta a_f}{a}, \quad \bar{\varepsilon}_{wp} = \frac{\Delta a_{wp}}{a} \qquad (2a), (2b)$$

Where,

$\bar{\sigma}_f$, $\bar{\sigma}_{wp}$: Mean axial stresses of the flange and the web panel

N_f, N_{wp}: Axial forces of the flange and the web panel in the middle of transverse stiffeners

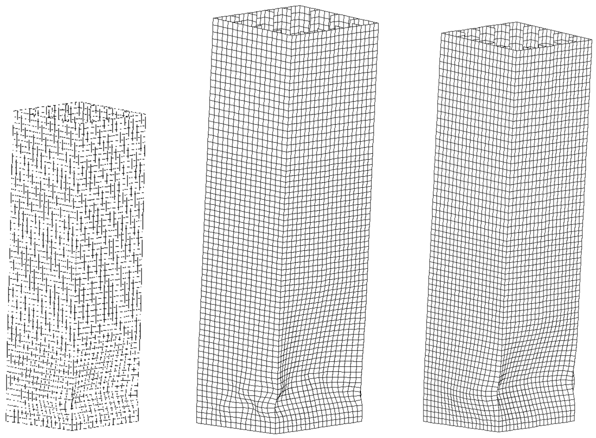

(a) C2 (b) C5 (c) C8

Fig. 2 Deformation shape of steel

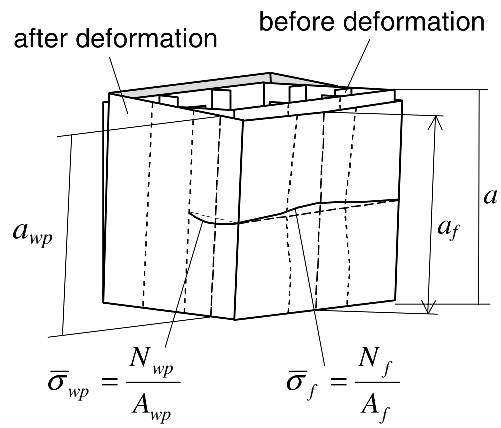

Fig. 3 Definition of the mean stress and

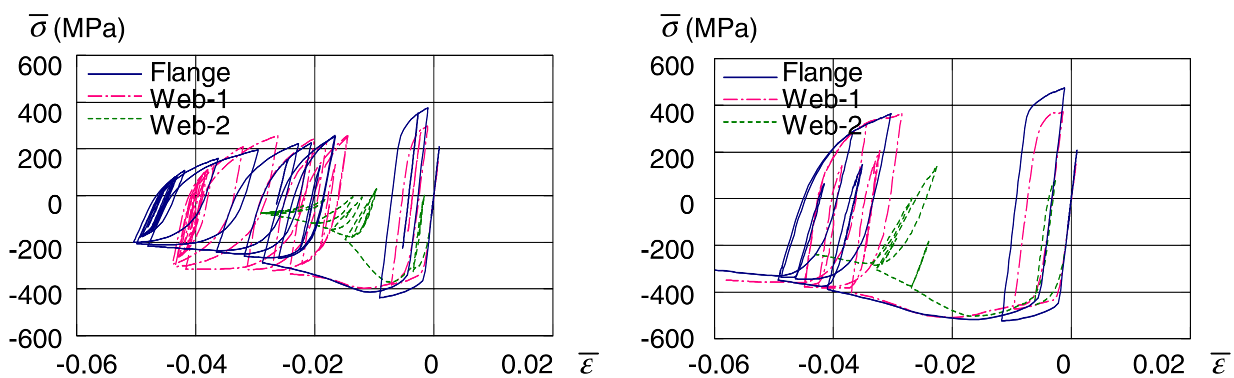

(a) C2 (b) C8

Fig. 4 Mean axial stress - strain relations of locally buckled stiffener spacing

A_f , A_{wp} : Sectional areas of the flange and the web panel in the middle of transverse stiffeners

$\overline{\varepsilon}_f$, $\overline{\varepsilon}_{wp}$: Mean axial strains of the flange and the web panel

Δa_f , Δa_{wp} : Change in the distance between transverse stiffeners at the flange and the web panel

$\Delta a_f = a_f - a$, $\Delta a_{wp} = a_{wp} - a$

a : Transverse stiffeners spacing

Fig. 4 shows the examples of the mean axial stress-strain relations of locally buckled stiffener spacing. The web panels are numbered from the panel adjacent to the buckled flange (**Fig. 5**). Furthermore, the absolute values of the buckling stress σ_{cr}, which is defined as the minimum value of the mean axial stress history $\overline{\sigma}_{min}$, are shown in **Table 2**.

The mean axial stress - plastic strain curves after local buckling, each being normalized by the value at buckling, are approximated by the least squares solutions as follows:

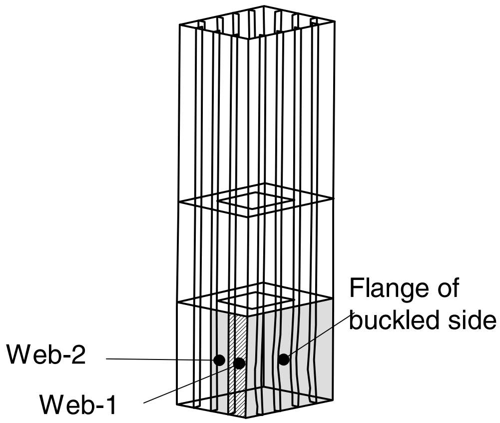

Fig. 5 Location of the output points of the mean stress and strain

Table 2 Local buckling stresses of steel columns

Column No.	Flange $\lvert\sigma_{cr}\rvert$ (MPa)	Web $\lvert\sigma_{cr}\rvert$ (MPa)	
		Panel-1	Panel-2
C1	508	496	487
C2	437	396	371
C3	440	398	390
C4	432	397	372
C5	427	415	-
C6	498	-	-
C7	299	294	256
C8	524	509	503
C9	439	416	376

$$\begin{cases} \text{Flange:} & \left(\dfrac{\bar{\sigma}}{\sigma_{cr}}\right)_f = \left\{1 + 10000\left(\bar{\varepsilon}_p - \bar{\varepsilon}_{pcr}\right)^2\right\}^{-0.25} & (3a) \\ \text{Web Panel-1:} & \left(\dfrac{\bar{\sigma}}{\sigma_{cr}}\right)_{w1} = \left\{1 + 46600\left(\bar{\varepsilon}_p - \bar{\varepsilon}_{pcr}\right)^2\right\}^{-0.14} & (3b) \\ \text{Web Panel-2:} & \left(\dfrac{\bar{\sigma}}{\sigma_{cr}}\right)_{w2} = \left(\dfrac{\bar{\sigma}}{\sigma_{cr}}\right)_f \left(\dfrac{\bar{\sigma}}{\sigma_{cr}}\right)_{w1} & (3c) \end{cases}$$

Unloading stiffness after local buckling

As the local buckling deflection increases, the unloading stiffness $\bar{E}$ of the flange or the web panel reduces from the initial value E_0. Additionally, the subsequent tensile yield stress $\bar{\sigma}_y$ takes smaller value than the initial value $\bar{\sigma}_{y0}$ (**Fig. 3**), which means that the elastic range becomes smaller.

The unloading stiffness - mean axial stress curves after local buckling, each being normalized by the value at buckling, are approximated by the least squares solutions as follows:

$$\begin{cases} \text{Flange:} & \dfrac{\bar{E}}{E_0} = \left(\dfrac{\bar{\sigma}}{\sigma_{cr}}\right)^2 & (4a) \\ \text{Web Panel-1:} & \dfrac{\bar{E}}{E_0} = \left(\dfrac{\bar{\sigma}}{\sigma_{cr}}\right)^{0.8} & (4b) \\ \text{Web Panel-2:} & \dfrac{\bar{E}}{E_0} = 1 - \sqrt{1 - \left(\dfrac{\bar{\sigma}}{\sigma_{cr}}\right)^2} & (4c) \end{cases}$$

FORMULATION OF BEAM ELEMENT CONSIDERS THE EFFECT OF LOCAL BUCKLING

For the sake of simplicity, we named here the transverse stiffener spacing where local buckling occurred in flanges or webs "plastic deterioration hinge (PDH)". The beam element for PDH will be formulated in this section.

The analysis results of the previous section indicate that the key features of the modeling of the mechanical characteristics of a PDH can be as follows:

i) Before local buckling, stress-strain relation follows kinematic hardening rule with strain hardening, and von Mises yield criteria ${\sigma_Y}^2 = \sigma^2 + 3\tau^2$ (Mises [11]) is applied.
ii) The local buckling stress of a flange is evaluated as the compressive elasto-plastic buckling stress of a T-section column whose array forms the flange.
iii) The local buckling stress of each panel in a web is evaluated as the elasto-plastic buckling stress of a simply supported panel subjected to a uniform axial compressive stress and an in-plane shear stress.
iv) The compressive buckling stress of a panel in a web will not get larger than that of the next panel previously buckled.
v) After local buckling, the elastic range isotropically contracts and its center keeps the position at buckling.

Fig. 6 shows the outline of the axial stress-strain curve of a PDH. For simplicity, the mean values $\bar{\sigma}$, $\bar{\varepsilon}$ and $\bar{E}$ will be rewritten hereafter σ, ε and E respectively, since the mean values will always be discussed.

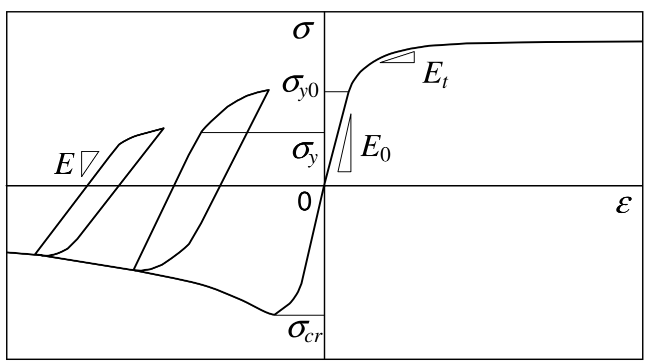

E_0: Initial elastic stiffness E_t: Tangential stiffness in plastic range E: Unloading stiffness
σ_{y0}: Initial yield stress σ_y: Subsequent yield stress σ_{cr}: Buckling stress

Fig. 6 Outline of the axial stress σ − strain ε curve of the beam element for PDH

Evaluation of flange local buckling stress using orthogonally-stiffened plate model
The orthogonally stiffened plate model (Nakai [12]) was used to evaluate the buckling stress of the stiffened flange plate. The buckling stress of a flange plate can be evaluated as the elasto-plastic buckling stress of the T-section column, whose array forms the flange, hatched in **Fig. 7**. The T-section column can be reasonably assumed to be fixed and pin-ended between the fixed end and the nearest transverse stiffener. In addition, it can be assumed both pin-ended between the transverse stiffeners.

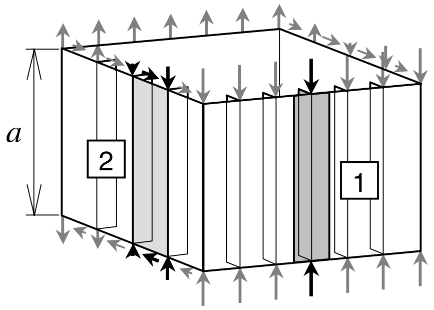

Fig. 7 Modeling for buckling stress evaluation

Table 3 Material constants

Steel types	C_1 (MPa)	C_2 (MPa)	σ_Y (MPa)	E_0 (GPa)
SM400A	264	162	250	206
SM490A	281	98.7	320	
SM490YA	263	-60.2	360	
SM490YB				
SM520B	305	36.4	360	
SM570	246	-94.8	455	

$$\sigma_{cr}^{T} = \begin{cases} \dfrac{2.04\pi^2 E_t I_T}{A_T a^2} & \text{(between the fixed end and the transverse stiffener)} \quad (5a) \\[2ex] \dfrac{\pi^2 E_t I_T}{A_T a^2} & \text{(between transverse stiffeners)} \quad (5b) \end{cases}$$

Where, I_T =moment of inertia of the T-section, A_T =area of the T-section, a =transverse stiffener spacing and E_t =tangential stiffness at buckling.

In the series of analyses here, the stress-plastic strain curves of the steel materials were approximated by the following equation.

$$\sigma = C_1\, \varepsilon_p^{\,1/4} + C_2\, \varepsilon_p + \sigma_Y \tag{6}$$

Consequently, the plastic modulus H_p and the tangential stiffness E_t are given by the following equations (Chen [13]).

$$\begin{cases} H_p = \dfrac{d\sigma}{d\varepsilon_p} = \dfrac{C_1}{4}\varepsilon_p^{\,-3/4} + C_2 & (7) \\[2ex] E_t = \dfrac{E_0 H_p}{E_0 + H_p} & (8) \end{cases}$$

Where, σ_Y = uniaxial yield stress of the material, C_1, C_2 = material constants and E_0 = initial elastic modulus. These parameters are shown in **Table 3**. C_1 and C_2 are the coefficients of the least squares solutions when the plots shown in **Fig. 1** are fitted by Eq. (6).

Evaluation of web local buckling stress using plate model

The buckling stress of a web panel can be approximated by the elasto-plastic buckling stress of a simply supported plate, which is hatched in **Fig. 7**, subjected to a compressive stress and a shear stress. It is assumed that each web panel is under uniform compression and shear, and the buckling condition is given by the following equation (Timoshenko [14]).

$$\frac{\sigma_{crw}}{\sigma_{cr}^{*}} + \left(\frac{\tau_{crw}}{\tau_{cr}^{*}}\right)^2 = 1 \tag{9}$$

Where, σ_{crw} = compressive stress at buckling, τ_{crw} = shear stress at buckling, σ^*_{cr} = elasto-plastic compressive buckling stress of simply supported plate under uniform compression and τ^*_{cr} = elasto-plastic shear buckling stress of simply supported plate under uniform shear.

Modeling of stress -strain relations after local buckling

It is assumed that the axial stress - plastic strain curves and the unloading stiffness - axial stress curves after local buckling are approximated by Eq. (3) and Eq. (4) respectively. Additionally, it is assumed that the yield surface keeps its position and isotropically contracts during compressive loading after local buckling.

Dividing and choosing elements

It should be noted that just one 2-node beam element should be used for transverse stiffener spacing, because the normalized stress-strain relation of PDH is used here. Additionally, Timoshenko beam element (Hinton [15]), which allows shear deformation, is used, because bending of thin steel members causes substantial shear stress in their webs.

VALIDATION OF THE PROPOSED MODEL

Time-history response analyses of box section steel piers were carried out to validate the proposed PDH beam element model. The dimensions and the analysis parameters of box-section piers are shown in **Table 4**. Two load cases were examined; the normal axial load ratio N/N_y and the larger value intended to ensure that local bucking occurs. The JMA acceleration history was imposed on pier bases.

Elasto-plastic finite displacement analyses were carried out using Newmark-β method (γ=1/2, β=1/4, Newmark [16]) for direct integration. The time increment was set to Δt=0.2msec.

Fig. 8 shows the deformed shapes of the piers with the large values of N/N_y calculated by the different models. The deformed shapes of the shell element model are shown as the side sectional views.

Table 4 Dimensions and analysis parameters of the box-section piers

No.	L (mm)	Flange			Web			Long. stiffener		Transverse stiffener			N/N_y‡ (%)	Steel type
		b_f (mm)	t_f (mm)	n_f	b_w (mm)	t_w (mm)	n_w	b_r (mm)	t_r (mm)	b_d (mm)	t_d (mm)	a† (mm)		
P1	7200	1600	38	3	1400	25	3	120	11	220	12	1800	5.6 (12)	SM490A
P2	10000	2000	25	5	1700	25	4	170	19	250	16	2000	9.3 (15)	SM570
P3	8600	1700	25	4	1700	16	4	140	14	230	15	1400	8.7 (15)	SM400
P4	7500	1700	19	4	1700	15	4	140	14	230	15	1500	11 (15)	SM490YA
P5	10500	2000	29	5	2500	29	5	140	14	270	17	1500	8.0 (15)	SM520B
P6	10700	2500	16	5	1600	16	3	130	12	240	16	2200	7.5 (12)	SM490A

† values at the bases
‡ values in parentheses are the larger ones than normal

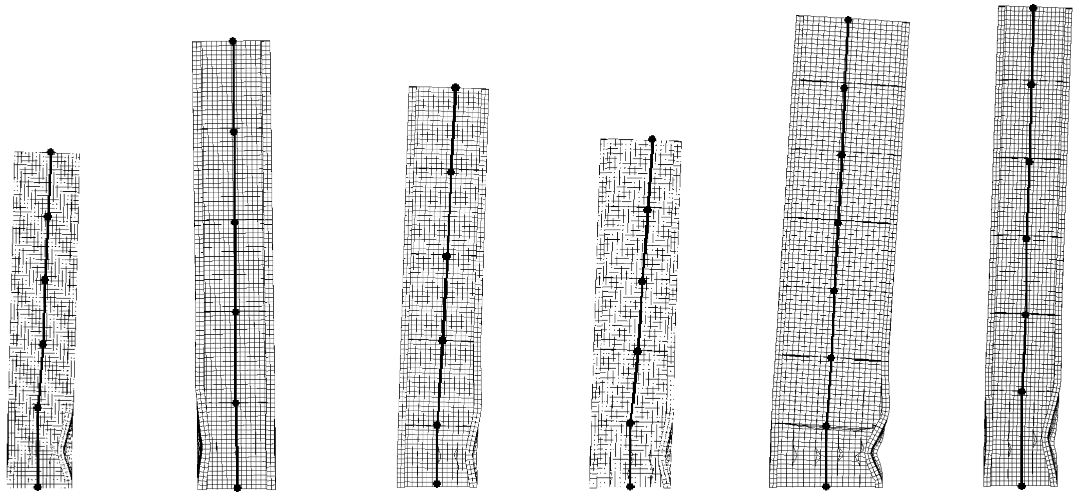

(a) P1 (b) P2 (c) P3 (d) P4 (e) P5 (f) P6

Fig. 8 Deformation of steel piers calculated by different FE models (Axial force ratios are larger than normal)

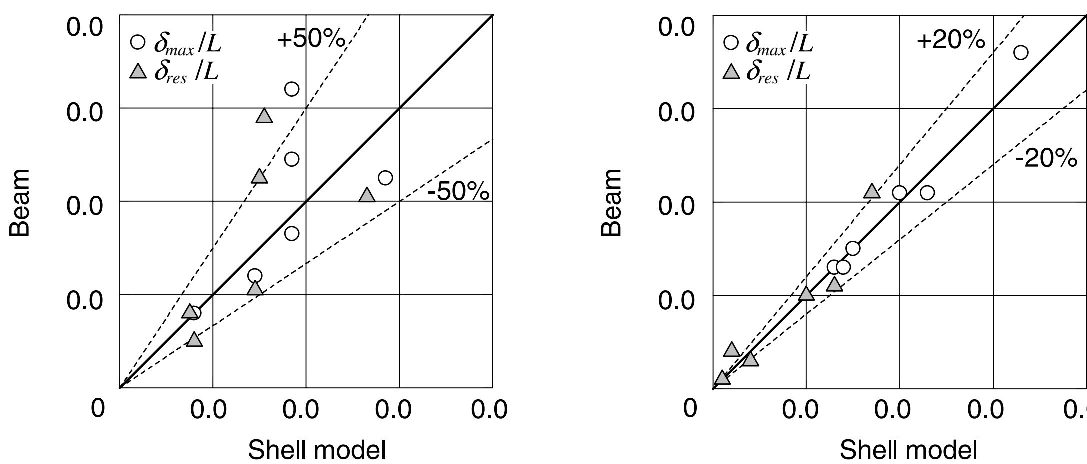

(a) Axial force ratios are larger than normal (b) Normal axial force ratios

Fig. 9 Comparisons of δ_{max} and δ_{res} of the steel piers calculated by different FE models

The maximum lateral displacement and the residual displacement of the pier tops were generally consistent with those calculated by FE analysis using shell elements (**Fig. 9**). However, it should be noted that webs of steel piers buckled as stiffened plate when (stiffener stiffness ratio) / (required stiffener stiffness ratio) (JSCE [7]) is around 0.6 and below, so that the beam element model overestimates the buckling stress of web plate. This is not negligible if the axial force ratio is bigger than usual, that is, around 15%.

APPLICATION TO A BOX SECTION STEEL RIGID FRAME

The proposed PDH model was applied to a time-history response analysis of a box section steel frame shown in **Fig. 10**. The rigid frame model was discretized to 19900 shell elements (1/2 model) or 35 beam elements. The JMA acceleration history was imposed on the bases perpendicular to the bridge axis.

Beam element discretization around a corner is illustrated in **Fig. 11**. The length of a beam element ℓ_i is defined as the sum of the transverse stiffener spacing a_i and the distance between the column edge (or the beam edge) and the center of the corner. The buckling stresses of the flange or the web panels are calculated using the transverse stiffener spacing a_i.

Fig. 12 shows the deformed shapes of the rigid frame calculated by the different models. In the shell FE analysis, local buckling occurred around the corner D, with three PDHs numbered in the figure. The dimensions of the PDHs are shown in **Table 5**.

No.	Reaction force (kN)
1	1069
2	899
3	476
4	514
5	1118
6	1182
7	913
8	1129

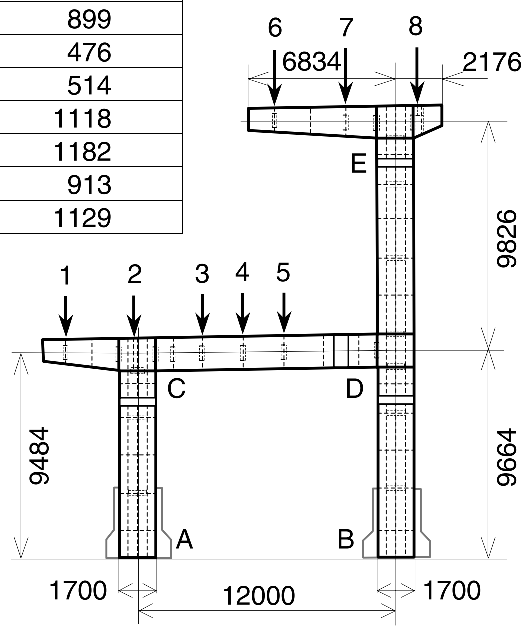

Fig. 10 Steel rigid frame

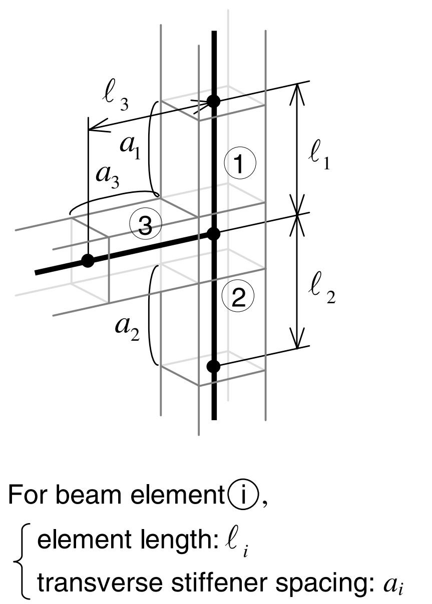

Fig. 11 Beam element discretization at a corner

Table 5 Dimensions of the PDHs in the rigid frame

PDH No.	Flange			Web			Long. stiffener		Transverse stiffener			Steel type
	b_f (mm)	t_f (mm)	n_f	b_w (mm)	t_w (mm)	n_w	b_r (mm)	t_r (mm)	b_d (mm)	t_d (mm)	a (mm)	
I	1700	25	4	1700	16	4	140	14	230	15	1800	SM400
II	1700	25	4	1700	16	4	140	14	230	15	1350	SM400
III	1700	22	4	1500	14	1	140	14	230	15	1744	SM490YA

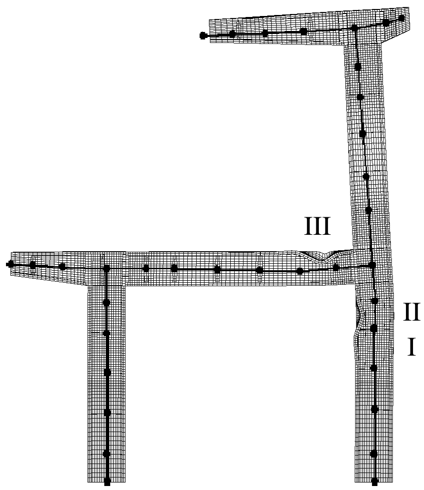

Fig. 12 Deformed shapes of the rigid frame calculated by different models (displacements scaled by a factor of 3)

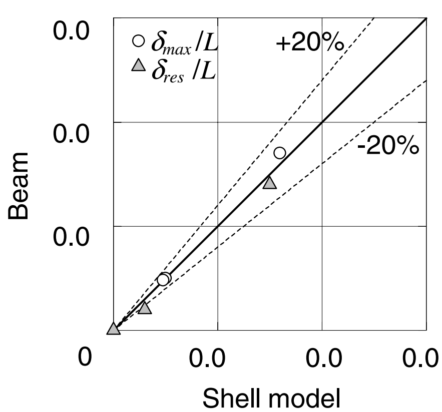

Fig. 14 Comparisons of δ_{max} and δ_{res} of the steel rigid frame corners

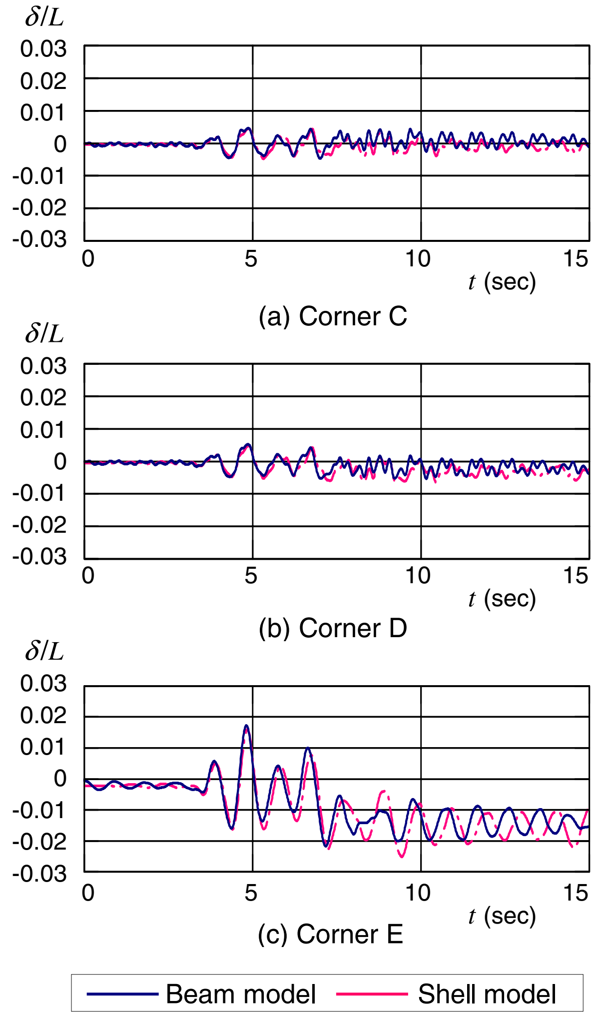

Fig. 13 Comparisons of the lateral relative displacement time histories of the rigid frame

The comparisons of the lateral relative displacement time histories of the corners are shown in **Fig. 13**. The maximum displacement and the residual displacement of the corners of the rigid frame were consistent with those calculated by FE analysis using shell elements (**Fig. 14**). Additionally, the axial stress-strain curves of PDHs were also well estimated by the beam model. As an example, the stress-strain curves of PDH II are shown in **Fig. 15**.

Analysis time was reduced to 8 minutes of the beam model from 120 hours of the shell model, when a workstation with sufficient memory was used.

These results show the effectiveness of the proposed beam element model for evaluating the maximum lateral displacement and the lateral residual displacement of box section steel frames.

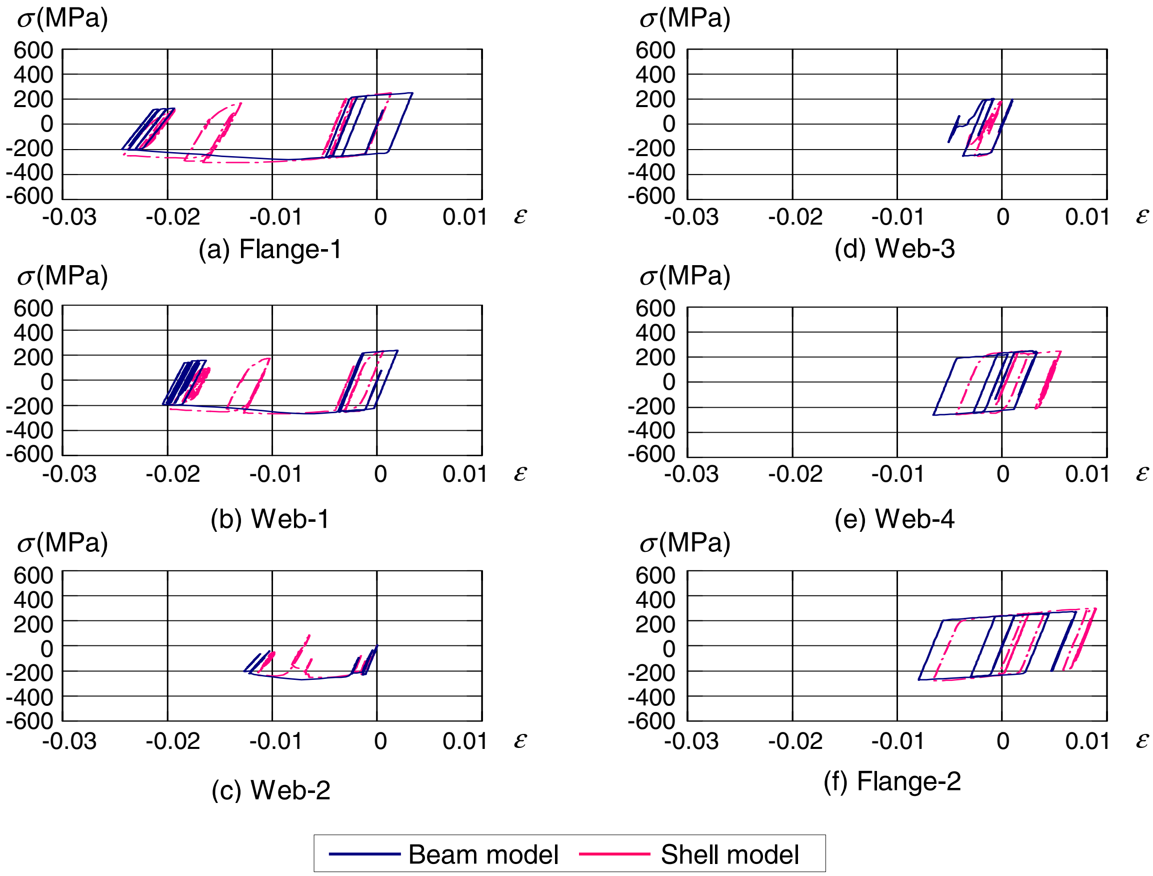

Fig. 15 Axial stress-strain curves of the rigid frame (PDH II)

CONCLUSIONS

A procedure for time-history response analysis intended to seismic diagnosis of existing box section steel frames in Japan was proposed and verified. Steel piers and frames were modeled by beam elements which consider the effect of local buckling. Conclusions are summarized as follows:

(1) FE analyses using shell elements show that local buckling of existing box section steel frames occurs practically between transverse stiffeners. Therefore, the average stress - strain relation of the beam element model, which considers the effect of local buckling, can be reasonably formulated for transverse stiffener spacing. It is formulated as a hardening and softening stress - strain relation for before and after local buckling occurs respectively. The buckling stress of flange was evaluated as the elasto-plastic buckling stress of T-section column, whose array forms the flange, subjected to an axial compressive stress. Furthermore, the buckling stress of web panel was evaluated as elasto-plastic buckling stress of simply supported panel subjected to a uniform axial compressive stress and an in-plane shear stress.

(2) One 2-node beam element should be used for one transverse stiffener spacing, because the averaged stress - strain relation of local buckling part is used in the beam σ–ε model. Furthermore, Timoshenko

beam elements or other beam elements that can model shear stress should be used, because bending of thin steel members produces substantial shear stress in their webs.

(3) The maximum displacement and the residual displacement of existing box section steel frames were well estimated by FE analysis using the beam element model that considers the deterioration effect due to local buckling, while the calculation time was considerably shorter than that of a shell element model. This model can be used for steel frames that have complicated shapes.

REFERENCES

1. JSCE. "Proposal on Earthquake Resistance for Civil Engineering Structures." 1996. (in Japanese, or http://www.jsce.or.jp/committee/earth/index-e.html for English version)
2. Japan Road Association. "Specifications for Highway Bridges Part V: Seismic Design." 1996.
3. for example, JSCE. "Proceedings of the 1st Symposium on Ductility Design Method for Bridges." 1998. (in Japanese)
4. Newmark N M, and Hall W J. "Seismic design criteria for nuclear reactor facilities." Proceedings of 4th World Conference on Earthquake Engineering, Chile, 1969: B5-1 - B5-12.
5. Oshima T, Mikami S, Ishikawa Y. "Stability of Nonlinear Bending Vibration Analysis of Pier Considering the Softening of M-ϕ Curve." Proceedings of the Third Symposium on Nonlinear Numerical Analysis and its Application to Seismic Design of Steel Structures, JSCE, 1997: 269-274. (in Japanese)
6. Isoe A, Ominami R, Yoshikawa T, Kishida K, Ishige T. "Development of a Simple Calculation Model to Simulate Behavior of Steel Box Column Piers under Cyclic Loads." Journal of Structural Mechanics and Earthquake Engineering, 1998; 42: 149-161. (in Japanese)
7. Japan Road Association. "Specifications for Highway Bridges Part I - Part II: Steel Bridges." 1996. (in Japanese)
8. Hibbitt, Karlsson & Sorensen, Inc. "ABAQUS/Standard User's Manual Version 5.8." 1998.
9. Japan Standards Association. "JIS Handbook Ferrous Materials & Metallurgy II." 1997.
10. JSCE Committee of Earthquake Engineering. "The 1995 Hyogoken-Nanbu Earthquake." 1996.
11. Mises R V. "Mechanik der plastichen Formanderung von Kristallen." Z.A.M.M., 1928; 8: 161-185. (in German)
12. Nakai H, Kitada T, Taido Y, Fukuoka S. "A Design Method of Orthogonally Stiffened Plates with Stringers under Uniaxial Compression." Journal of Structural Engineering, JSCE, 1985; 31A: 103-114. (in Japanese)
13. Chen W F, Han D J. "Plasticity for Structural Engineers." Springer-Verlag, New York, 1988.
14. Timoshenko S P, Gere J M. "Theory of Elastic Stability (Second Edition)." McGraw-Hill, New York, 1961.
15. Hinton E, Owen D R J. "Finite Element Programming." Academic Press, New York, 1977.
16. Newmark N M. "A Method of Computation for Structural Dynamics." Journal of the Engineering Mechanics Division, Proceedings of the ASCE, 1959; 85: 67-94